# A Cartographic Modeling Approach for Surface Orientation-Related Applications

Michael E. Hodgson and Gary L. Gaile

## Abstract

*Applications requiring the comparison of angular directions, descriptive angular statistics, or spatial interpolation of directional data are problematic to implement because accepted GIS modeling language constructs do not contain the directional data types or operators. Embedded directional operators or models may be developed with existing GIS functionality by reorganizing the directions into unit vectors. Representation of directional observations, such as surface orientation or solar rays, in a unit vector matrix form allows for the development using linear algebra in cartographic modeling constructs. This article presents fundamental directional operators and demonstrates their development for several surface-oriented applications: mean and dispersion in neighborhood surface orientation, comparison of surfaces, shaded relief mapping, topographic normalization of remotely sensed imagery, and solar radiation. Extension of the fundamental directional operators to spatial interpolation is also discussed.*

## Introduction

Modeling of topographic surfaces and the effects of topography on other variables is a prevalent topic in many environmental modeling applications. Many of these disparate applications require not merely independent treatment of elevation or slope/aspect angles, but also treatment of the bidirectional angle that describes surface orientation. Examples of such applications include mapping shaded relief, modeling solar radiation, topographic normalization of remotely sensed imagery, or comparison of two different digital elevation models (DEMs) of the same area. Other applications need directional statistics to analyze measures of central tendency and dispersion in surface orientation angles. Modeling of many environmental processes requires the use of what some have called vector fields (Kemp, 1992), such as wind flow or even surface slope/aspect. Finally, although spatial interpolation of scalar fields is common in geostatistics, spatial interpolation of vector fields is problematic in a GIS.

Models constructed for topographic surface orientation applications share the unique problem of representing the bidirectional angle (i.e., slope and aspect together) of a surface and of comparing the bidirectional surface angle with other three-dimensional angles. The *bi*directional angle is different from the *uni*directional angle (i.e., aspect alone) associated with surface water flow or surface winds. The bidirectional *surface* angle is almost 3D but is limited to the two-and-one-half dimensions of hemispherical space. However, in applications it may be used in comparisons with either other hemispherical angles or 3D angles, such as other surface angles or solar rays, respectively. Unfortunately, modern GISs or image processing systems do not include either a bidirectional *data type* (e.g., a mathematical vector data type) or the bidirectional *operators* with which to efficiently construct topographic surface orientation-related models[1]. Only recently were vector data types introduced in a modern GIS (i.e., ESRI's ArcView vector data object). In addition, modern GISs, image processing systems, or even statistical packages do not include procedures for deriving the *directional statistics* that characterize a set of bidirectional surface angles. The authors view this deficiency as a *conceptual impediment*—not a technical impediment. This article presents the constructs for fundamental directional operators that may be used to construct models for the applications described above. In a departure from previous work in these applications, (1) the angles are represented as unit vectors, (2) the operators are based on linear algebra, and (3) the implementation is entirely with existing cartographic modeling constructs. Representing and analyzing the directional nature of surface orientation in this manner provides a common foundation for a wide variety of surface analyses and directional statistics related applications.

This article describes an *embedded* approach to modeling the bidirectional nature of surfaces using *cartographic modeling* concepts and *linear algebra*. For example, two categories of surface orientation applications are presented: (1) directional statistics and (2) surface-normal solar-ray models. Extension of these fundamental directional statistics to spatial interpolation is then presented. The intent here is to demystify the nature of such functions or models and to place the conceptual measurements/statistics in an accepted GIS modeling language framework. Primitive operators for unit vectors in matrix algebra are first developed and provide the common link between surface-orientation directional statistics and surface-normal solar-ray models. The fundamental applications and formulae requiring the hemispherical treatment of topographic surfaces are then presented. Following the "cartographic modeling" concept by Tomlin (1990), each application is implemented using local, neighborhood, and zonal operators in three-dimensional vector algebra notation. Finally, these cartographic modeling-based operators are summarized in a proposed set of standard directionally related objects and operators. The intent is not to review the theoretical arguments and empirical results for various topo-

[1] To the authors' knowledge, directional data types and associated operators do not exist in any of the raster-based commercial GIS or remote sensing packages.

M.E. Hodgson is with the Department of Geography, University of South Carolina, Columbia, SC 29208.

G.L. Gaile is with the Department of Geography, University of Colorado, Boulder, CO 80309.

Photogrammetric Engineering & Remote Sensing,
Vol. 65, No. 1, January 1999, pp. 85–95.

0099-1112/99/6501–0085$3.00/0

TABLE 1. PRIMITIVE DIRECTIONAL OPERATORS AND MODELS BASED ON DIRECTIONAL OPERATORS

| Primitive Directional Operators | Models and Directional Operators Needed |
|---|---|
| Unit Vector for Surface or Sun | Surface Orientation Comparison<br>Unit Vector, Spherical Angle |
| Spherical Angle between Vectors | Surface Neighborhood Characterization<br>Unit Vector, Mean Unit Vector, Dispersion |
| Mean Unit Vector | Surface Zonal Characterization<br>Unit Vector, Mean Unit Vector, Dispersion |
| Dispersion in Unit Vectors | Shaded Relief Mapping<br>Unit Vector, Spherical Angle |
| | Topographic Normalization: Lambertian<br>Unit Vector, Spherical Angle |
| | Topographic Normalization: Non-Lambertian<br>Unit Vector, Spherical Angle |
| | Solar Radiation<br>Unit Vector, Spherical Angle |
| | Interpolation of Directional Data<br>Unit Vector, Mean Unit Vector |

graphic normalization, directional statistics, solar radiation models, and spatial interpolation. With the exception of spatial interpolation of directional data, several others have conducted excellent work in these areas and the appropriate references are included for the reader. The purpose of this article is to provide the fundamental operators and procedures common to these models so that others can easily construct a variety of such models and continue improving on their use and development.

## Coupled and Embedded Operators/Models

Solutions to topographic surface orientation include (1) coupling between GIS and existing non-GIS models/statistical packages, (2) embedding "black-box" GIS functions/models, or (3) embedding the application using a GIS modeling language (Wesseling *et al.*, 1996). Coupling of external models is often used in topographic surface analysis, such as surface form characteristics (Gallant and Wilson, 1996). The advantage of coupling is to reuse complex models or operators that have already been implemented. Coupling approaches often suffer from the inherent incompatibility of confidential file structures (e.g., Arc/Info's spatial data, ERDAS Imagine's *.img* grid data) in the "coupled" applications. Thus, conversion of file structures between the GIS and the coupled model and back is normally required. A "black-box" model or operator is one embedded within the GIS but whose formula, algorithm, and details are occasionally hidden (e.g., proprietary). "Black-box" approaches are convenient for a specific use but prevent any modification and obscure the exact functional linkages. Furthermore, if the algorithms are hidden in either external coupled models or "black-box" operators, their evaluation or use in error propagation and uncertainty is confounded.

An ideal solution for surface oriented related operators or models would be an embedded approach using the *conceptual constructs* in either an ANSI or *defacto* standard GIS modeling language (Wesseling *et al.*, 1996; Zhang and Griffith, 1997). To date, the high-level modeling constructs in the cartographic modeling language (Tomlin, 1990) or map algebra language (Tomlin and Berry, 1979; Berry, 1987) are the closest to a high-level *defacto* standard for GIS modeling language. An embedded model is developed within the GIS using existing functionality through scripting or macro languages. In general, the dominant raster-based GISs have adopted the local, focal, and zonal formalizations in the cartographic modeling language by Tomlin (1990). This cartographic modeling functionality is available directly through the command language (e.g., Arc Grid), the graphical user interface (GUI), the graphical modeling language (e.g., ERDAS Spatial Modeler), or through the scripting language (e.g., Avenue, ERDAS macro language). A model that adheres to the formalizations in cartographic modeling will be more universal across GISs, more stable over time, and, thus, more portable and easier to maintain. By using the existing GIS constructs of a modeling language, the surface orientation models could be modified, encapsulated as functions, documented, used for error/uncertainty propagation, and presented in educational form. Some specific applications presented here, such as solar radiation modeling, have embedded the conceptual model in a macro language such as AML (Dubayah and Rich, 1995) or Spatial Modeler.

We believe that the implementation of the directional operators and vector statistics is possible with the *existing* GIS data models and functions. If such implementation is possible, then previously noted impediments to such directional-based modeling is a *conceptual problem*—not a technical problem.

## Categorization of Applications

The two applications—surface orientation and surface-sun angular relations—make use of the two fundamental measurements of surface orientation and solar position—slope and aspect or solar elevation and solar azimuth. Seven algorithms for estimating slope and aspect have been presented elsewhere (Sharpnack and Akin, 1969; Ritter, 1987) and compared (Skidmore, 1989; Hodgson, 1998). At least one of these algorithms for deriving slope and aspect is built into all GISs as a "black-box" command or operator. In the cartographic modeling language constructs, these operators are expressed as *focal* operators with *immediate neighborhoods* (i.e., using a 3 by 3 window). Although not explicitly presented in this article, implementing any of the various slope/aspect algorithms using the vector algebra and cartographic modeling constructs discussed in this article is possible.

Once these slope and aspect characteristics are derived, then other higher-order operators or models of processes are created. The surface orientation and surface-sun applications are both easily implemented using mathematical directional operators (Table 1). Other higher-order operators may be built using these primitives, and, ultimately, models may be constructed.

Specific implementation of these models, such as topographic normalization or solar radiation, often use spherical trigonometry. Other formulae for directional statistics often rely on the use of complex numbers (e.g., Hanson *et al.*, 1992; Klink, 1998). Complex data types are not common in GIS, presenting an implementation impediment. Compared to previous work, all of the *hemispherical* angular measurements in this article are based on unit vectors and linear algebra. The use of unit vectors and linear algebra provides a common foundation for developing the operators above and constructing these and other models. By characterizing surface orientation as a unit vector, both directional statistics for surfaces and solar-radiation related models may be implemented using existing constructs in cartographic modeling: scalar data types and local, focal, and zonal operators. In keeping with the broader concept of cartographic modeling, more complex operations or models can be built on a *logical structuring* of these cartographic modeling primitives. For example, a model of instantaneous solar radiation will be constructed from the angle between local vectors, which are in turn constructed from local vector components. Furthermore, the use of linear algebra, as compared with spherical trigonometry, provides a useful instructional base as it is familiar to most students.

Implementation of the formulae for the statistical or process models described above is accomplished through a set of conventions. After presenting each formula, the implemented model will follow the following translation of the mathematical formulae to cartographic modeling primitives:

$\vec{\mathbf{T}}_i$ and $\vec{\mathbf{S}}$ are unit vectors,

where $\vec{\mathbf{T}}_i$ is normal to the surface at cell$_i$ and $\vec{\mathbf{S}}$ points toward the sun;

$\sum$ implies summing the observations in a neighborhood (i.e., focal operator) or zone (i.e., zonal operator); and

$\int dH$ implies integration by approximation using a local sum operation for each observation in time (e.g., by hour).

## Primitives

The vector normal to the terrain surface ($\vec{\mathbf{T}}_i$) is represented as a matrix containing the vector endpoint. The implied origin is at the center of the cell and of unit length (i.e., length of 1.0 units) (Figure 1a): i.e.,

$$\vec{\mathbf{T}}_i = [x, y, z] \tag{1}$$

where

$x = \sin(\text{aspect}) * \sin(\text{slope})$, or $x = 0.0$ if slope $= 0.0$
$y = \cos(\text{aspect}) * \sin(\text{slope})$, or $y = 0.0$ if slope $= 0.0$
$z = \cos(\text{slope})$

The unit vector used here implies direction but not magnitude. As will be seen later, representation of the surface orientation as a 3D vector obviates the problems of including observations with a slope of 0.0 degrees, or undefined aspect. This consideration is important for including all observations in a zone when deriving mean and dispersion in surface orientations (Hodgson and Gaile, 1996).

The embedded cartographic modeling implementation creates three separate grid layers of the $x$, $y$, and $z$ components of the normal vectors (Figure 2). Using a local operator, the vector endpoint components are derived from Equation 1. These three grids are the foundation for developing all other operators presented here.

To derive the three-dimensional angular difference between two vectors pointing away from the same origin (Figure 1b), the dot product of two vector matrices is used. The cosine of the angle between two vectors is equivalent to the dot product of the two vectors divided by the product of the vector lengths: i.e.,

$$\cos(i) = \frac{\vec{\mathbf{T}} \cdot \vec{\mathbf{S}}}{|\vec{\mathbf{T}}|\ |\vec{\mathbf{S}}|}\,. \tag{2}$$

Because the vectors are of *unit* lengths (i.e., always equal to 1 unit in length), the denominator of Equation 2 is 1.0 and Equation 2 may be simplified to

$$\cos(i) = \vec{\mathbf{T}} \cdot \vec{\mathbf{S}} = t_x * s_x + t_y * s_y + t_z * s_z\,. \tag{3}$$

## Comparison of Surface Form

A common methodology for accuracy assessment in remote sensing and GIS DEM generation studies is to compare the surface derived from a specific technique (e.g., softcopy photogrammetry) to a reference data surface for the same study area. The reference data approximates "truth." Often the reference data are samples of the surface (Bolstad and Stowe, 1994) while other studies use reference data of the entire surface to be examined (Hodgson, 1995). The common practice in the accuracy assessment is to conduct separate evaluations of the errors in elevation, slope, and aspect. Evaluating errors in bidirectional orientation could also be conducted by comparing the bidirectional surface orientation angles of the test surface with the reference surface (Hodgson, 1998). This comparison involves two angles in one hemisphere rather than the full three-dimensional case as the surface element in a DEM cannot point "down" (Figure 1b). Knowledge of the errors in surface orientation is more important for applications where solar radiation or topographic normalization will be conducted. Few studies have used such a comparison method, presumably because of the lack of GIS tools for comparing hemispherical angles.

Using cartographic modeling concepts, the angle between the two vectors (Equation 3) is computed from the $x$, $y$, and $z$ components of each vector derived in Equation 1. In this application, the two vectors represent the surface orientation for the same cell in surface 1 and surface 2. These surface normal vectors from the two surfaces are referred to as $\vec{\mathbf{T}}_1$ and $\vec{\mathbf{T}}_2$. The angle between the two vectors is computed as in Equation 3.

Implementation of the bidirectional angular difference is illustrated using cartographic modeling constructs in Figure 3a. Once the $x$, $y$, and $z$ components of the vector in each cell are computed as separate map layers, the hemispherical angular difference ($i$) is derived using a local operator. The local operation is an implementation of Equation 3, the dot product of two vectors.

## Mean and Dispersion in Surface Orientation

A common conceptual measure for either remotely sensed imagery or landscape data is to characterize the neighborhood variability and central tendency. Example measures of central tendency are mean brightness values in imagery, median landcover class, average slope, or "average" aspect. The "average" hemispherical surface orientation and dispersion in hemispherical angles analogous to the mean and standard deviation in linear statistics can be devised using directional statistics and are presented in greater detail elsewhere (see, for example, Gaile and Burt (1980), Mahan (1991), and Hodgson and Gaile (1996)). The fundamentals for directional statistics were developed over 100 years ago (Rayleigh, 1880) but are seldom utilized in GIS, presumably due to the lack of any available GIS functionality. As indicated earlier, even statistical packages that might be "coupled" with a GIS do not contain the relevant directional statistics.

If the $x$, $y$, and $z$ components of the vector normal (i.e., $\vec{\mathbf{T}}_{\text{sum}}$) for each cell in an $n$ by $n$ neighborhood (e.g., a 3 by 3 window) has been derived, the mean vector is

$$\vec{\mathbf{T}}_{\text{sum}} = \sum \vec{\mathbf{T}}_i = [x_{\text{sum}}, y_{\text{sum}}, z_{\text{sum}}] \tag{4}$$

where each $\vec{\mathbf{T}}_i$ is the surface normal for a grid cell in the neighborhood (Figure 1c).

Computing a mean surface slope for the neighborhood is derived from a ratio of the length of the projected vector on the $x$-$y$ plane and the $z$ component of the vector: i.e.,

$$\text{Slope}_{\text{mean}} = \tan^{-1} \frac{\sqrt{x_{\text{sum}}^2 + y_{\text{sum}}^2}}{z_{\text{sum}}}\,. \tag{5}$$

The mean aspect is derived algorithmically from the signs and ratio of $x_{\text{sum}}$ and $y_{\text{sum}}$ (e.g., Ritter, 1987). Measures of dispersion in the 3D vectors of a neighborhood, analogous to variance and standard deviation in linear statistics, may also be computed. The hemispherical "variance" ($S_h$) and hemispherical "standard deviation" ($s_h$) are derived from the length ($R_h$) of the vector $\vec{\mathbf{T}}_{\text{sum}}$: i.e.,

$$R_h = |\vec{\mathbf{T}}_{\text{sum}}| \tag{6}$$

$$S_h = 1.0 - \frac{R_h}{N} \tag{7}$$

$$s_h = \sqrt{2.0 * (1 - \frac{R_h}{N})} * \frac{180}{\pi} \tag{8}$$

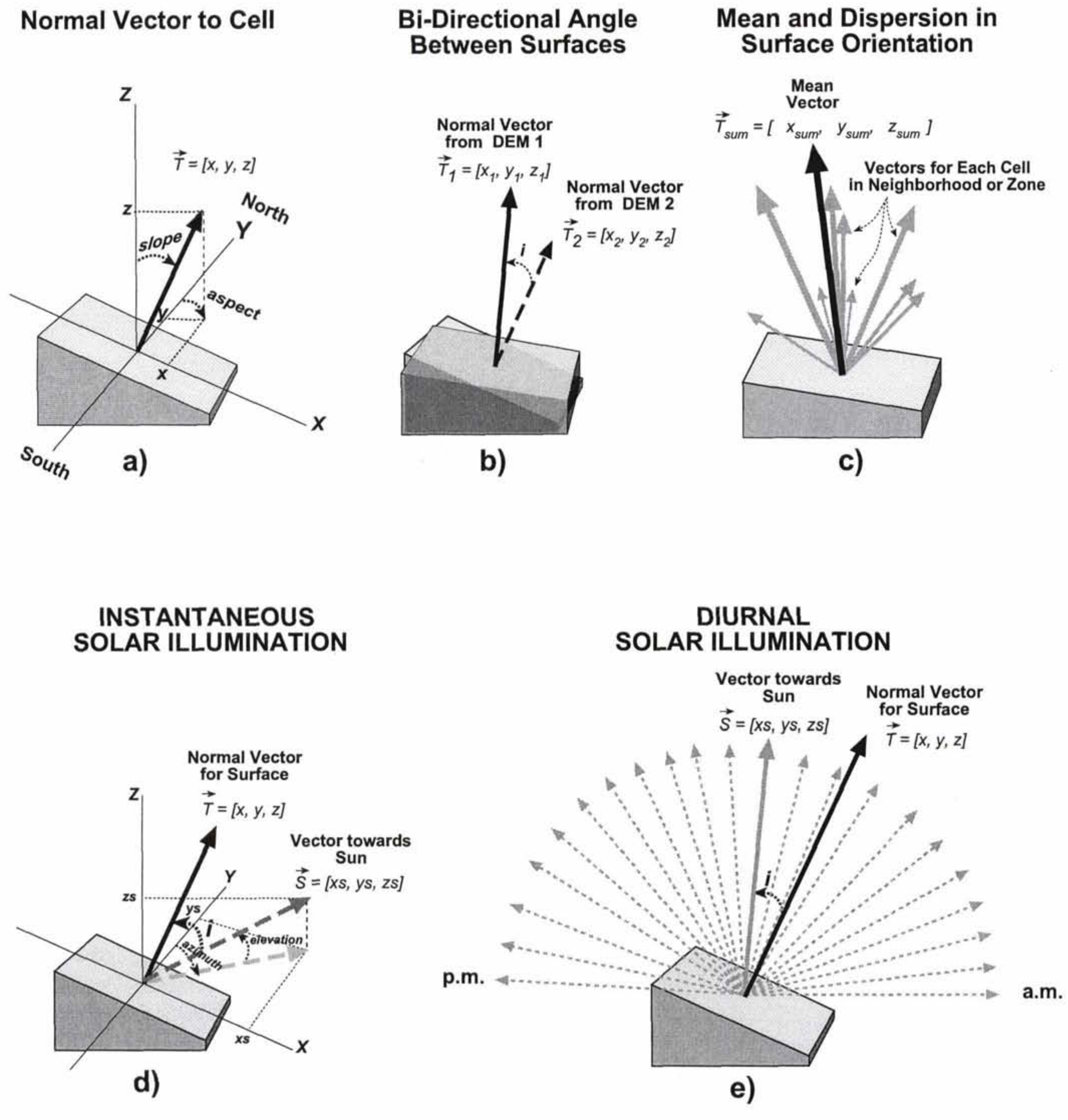


Figure 1. Fundamental representation of surface-related directions and operators. The three-dimensional vector normal to a surface slope is shown in (a). Three-dimensional angle between two unit vectors normal to each surface is shown in (b) and the mean and dispersion in a set of surface normals is shown in (c). The specification and relationship between the surface normal and solar rays is shown in (d) while the instantaneous solar rays and surface normal are shown in (e).

The number of cells in the neighborhood is $N$. As compared to its linear analog (i.e., variance) that can have any positive value, $S_h$ only varies from 0 to 1. Interpretation of the hemispherical "standard deviation" ($s_h$) is similar to the interpretation of standard deviation in linear statistics.

The implementation of Equation 4 is with three separate *focal* cartographic modeling operations using the surface normal vectors ($\mathbf{T}_i$) from each surface element in an extended neighborhood (Figure 3b). The vector matrix values are the sums of the respective $x$, $y$, or $z$ components in the neighborhood. Implementation of Equations 6, 7, and 8 only requires the traditional local map algebraic operations in cartographic

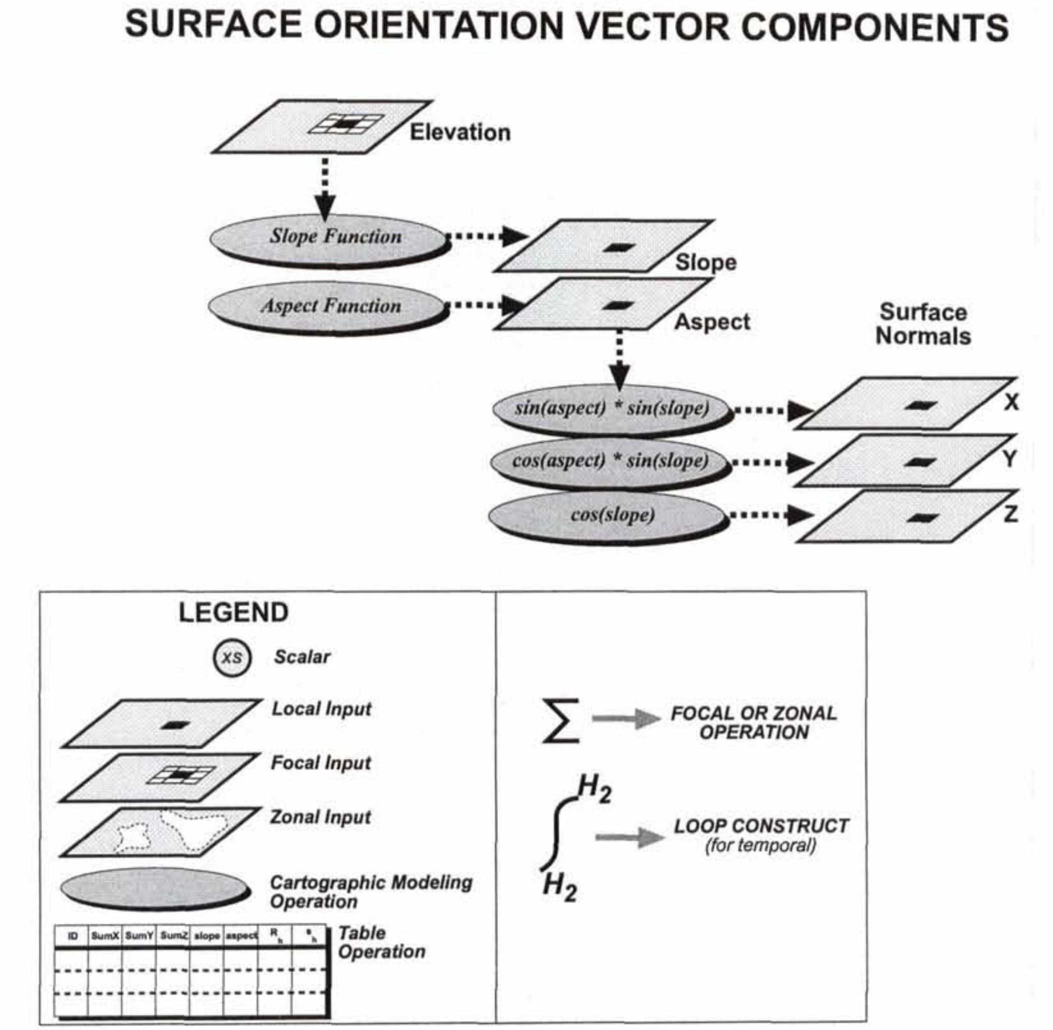


Figure 2. Computation of the three components (i.e., *x*, *y*, and *z*) for the surface normals in a map layer. Conceptually, this set of cartographic modeling operations could be encapsulated as a single operator — *Vcomponents*.

modeling. The entire implementation is presented in Figure 3b.

Extension of the neighborhood mean and dispersion in surface orientation to *zones* is straightforward (Figure 3c). Rather than using focal operators to sum the *x*, *y*, and *z* components of the vectors in a neighborhood, a zonal operator is used along with a map layer describing the zones. The implementation of Equations 6, 7, and 8 for mean slope, "variance," and "standard deviation" in surface orientation angles within a zone may be computed using tabular operations (Figure 3c). The value of $N$ varies by zone and is equivalent to the number of cells within the zone.

## Shaded Relief Mapping

The objective of shaded relief mapping is to simulate the appearance of the topographic surface in planimetric form caused solely by the variation in illumination due to bidirectional surface orientation with respect to the sun's rays (Figure 1d). Practically all modern GISs contain one shaded relief model as a "black box." The standard shaded relief model varies the apparent brightness of the terrain unit as a linear function of the angle of incidence ($i$) between the solar rays (vector $\mathbf{S}$) and surface normal (vector $\mathbf{T}$): i.e.,

$$\cos(i) = [\vec{\mathbf{T}} \cdot \vec{\mathbf{S}}] = [x * xs + y * ys + z * zs] \qquad (9)$$

where

$\mathbf{S} = [xs, ys, zs]$, the vector representing solar rays;
$xs = \sin(\text{solar azimuth}) * \sin(90 - \text{solar elevation})$;
$ys = \cos(\text{solar azimuth}) * \sin(90 - \text{solar elevation})$; and
$zs = \cos(90 - \text{solar elevation})$.

For maps of small portions of the Earth, the orientation of the solar rays (i.e., vector $\mathbf{S}$) is constant for the entire map. The surface normal for each grid cell, however, varies throughout the study area. Except for the constant solar angles, computation of the angle between the two vectors in Equation 9 is identical to that in Equation 3. Cells with a negative $\cos(i)$ are in self-shadow. On a shaded relief map, the brightest cells are those with a large value of $\cos(i)$. The apparent brightness is then normally scaled from 0 to 255 (i.e., dark to light) by multiplying the cosine of $i$ by a constant for the maximum brightness (e.g., 255): i.e.,

$$\text{Brightness} = \cos(i) * 255 \text{ if } \cos(i) \geq 0, \quad \text{or} \qquad (10)$$
$$\text{Brightness} = 0 \text{ if } \cos(i) < 0.$$

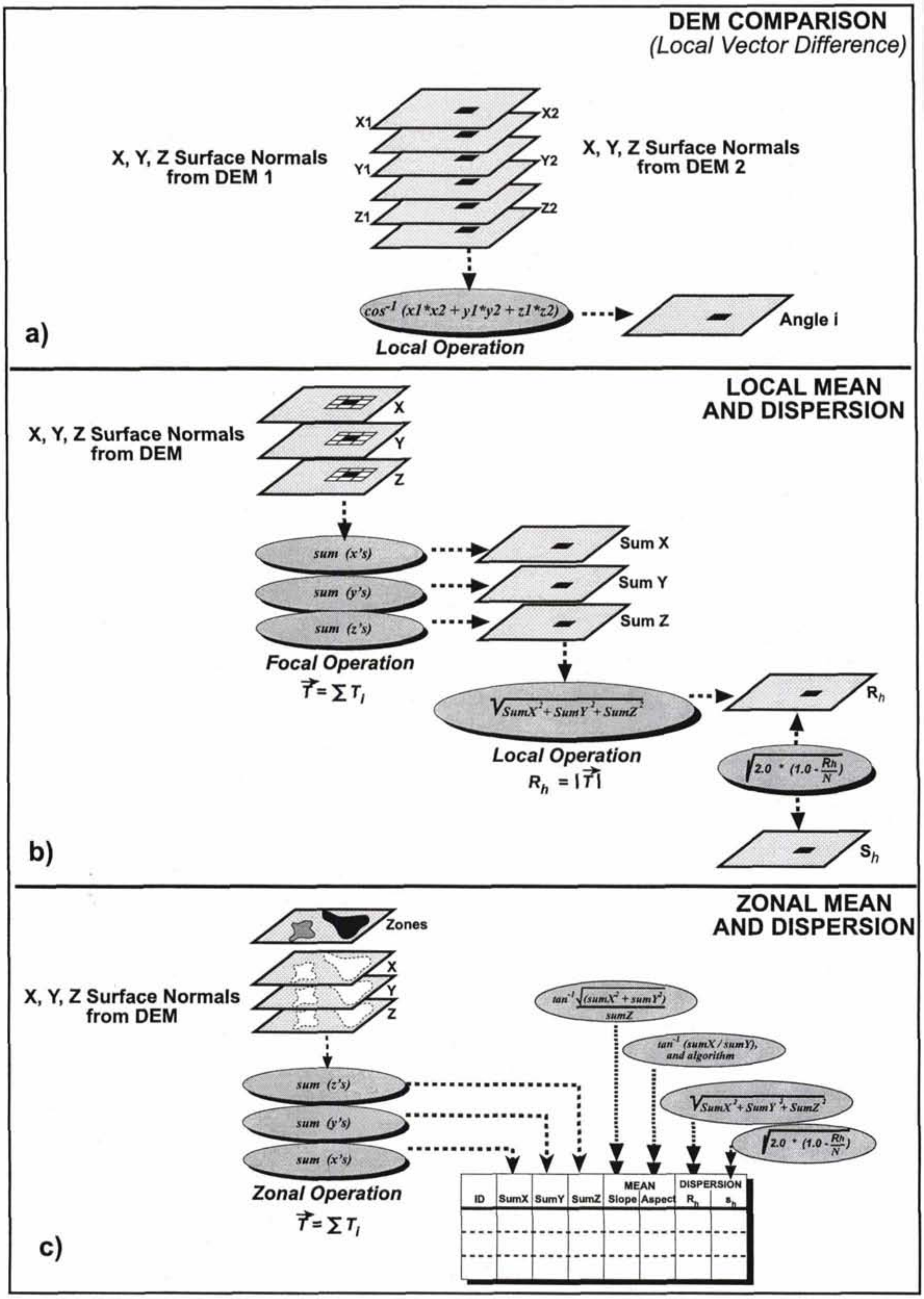


Figure 3. Fundamental cartographic modeling operations on a grid of surface normal vector components to produce the difference between two surface normals (a), and the mean and dispersion in surface normals of a neighborhood (b) and a zone (c). The operations in (a) might become a *localVdiff* operator. The neighborhood mean and dispersion primitives might become the *focal _ Vmean* and *focal _ Vstd* operators while the zonal primitives might be *zonal _ Vmean* and *zonal _ Vstd.*

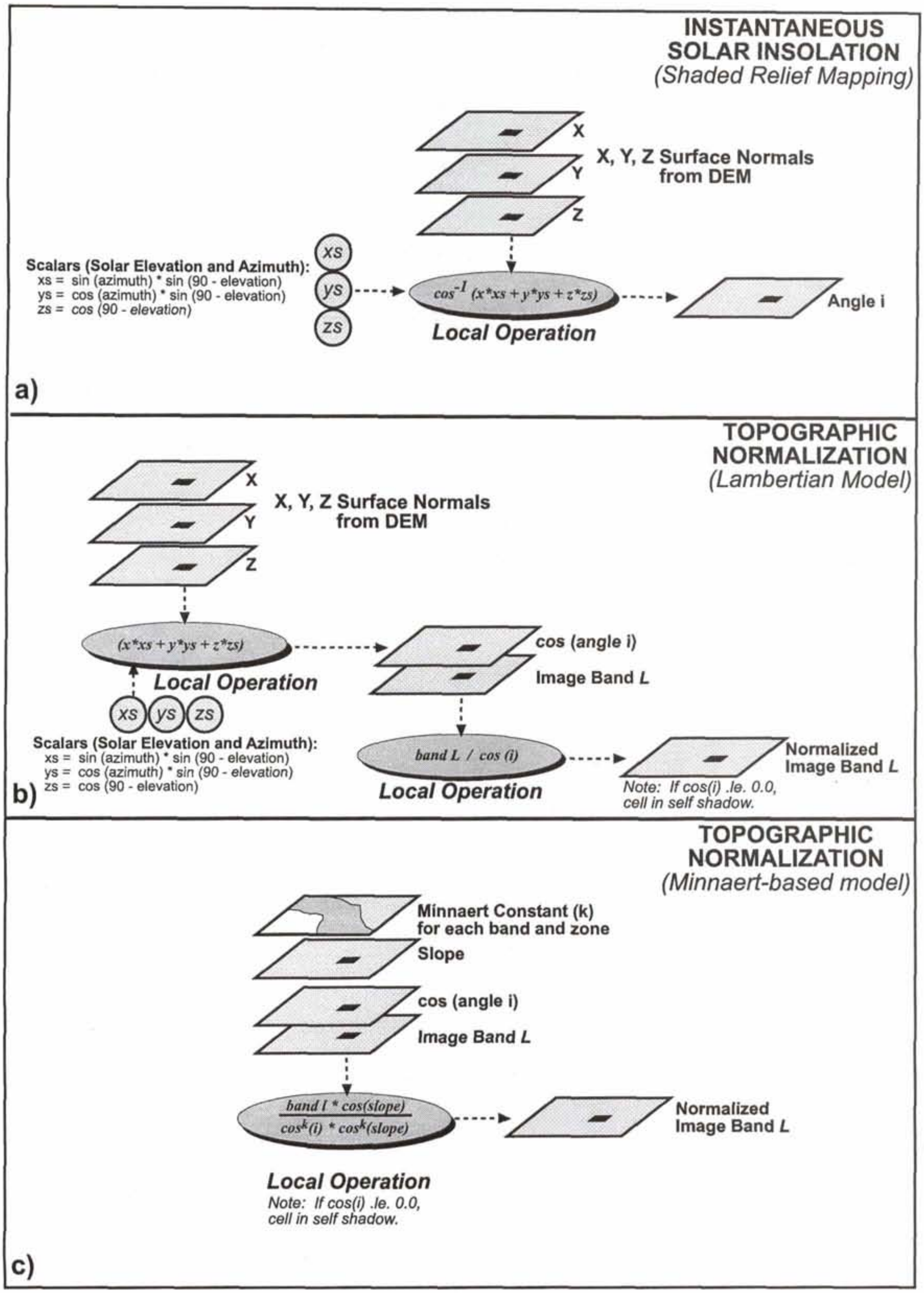


Figure 4. Fundamental cartographic modeling operations for deriving the instantaneous solar radiation on a surface are shown in (a) and for normalizing remotely sensed imagery using a Lambertian and Minnaert-based models are shown in (b) and (c), respectively.

The cartographic modeling implementation uses the map layer of vector endpoints (Figure 2) and two scalars for solar elevation and aspect (Figure 4a). The model then adds one local operator to derive *i*. By implementing the shaded relief mapping directly in cartographic modeling, the analyst may easily implement a non-Lambertian reflectance model (i.e., described below) or make modifications for haze and cloud shadows. The surface represented by $i$ could also be used to develop the "shadowed contours" presented by Yoeli (1983). This general concept for predicting the angle of incidence could also be extended to predict "hot spots" on imagery of water bodies where the map layer of **T**$s$ represents view angles from the surface to the sensor.

## Topographic Normalization

The objective in topographic normalization is to remove or minimize the variation in illumination in a remotely sensed image caused solely by the variation in surface orientation to the solar rays. Thus, the objective in topographic normalization is the inverse of that in shaded relief mapping. The remote sensing community has generally made use of three models for topographic normalization — Lambertian model (Holben and Justice, 1980), Minnaert model (Smith *et al.*, 1980; Colby, 1991), and a two-stage normalization model (Civco, 1989). Presentation of the merits of each is beyond the scope of this article. For in-depth reading, the references above are provided. All three models use the angle of incidence ($i$) between the surface normal and solar rays as defined above (Equation 9). All three models assume that the raw reflectance values have been transformed to radiance ($L_\lambda$) and the diffuse atmospheric component (i.e., skylight) has been removed. Transformation to radiance is accomplished by means of a simple table look-up. Removal of the atmospheric component is often accomplished using black body subtraction (Jensen, 1996).

Assuming a Lambertian surface, the form of the topographic normalization model is

$$Ln_\lambda = \frac{L_\lambda}{\cos(i)} \tag{11}$$

where $Ln_\lambda$ is the normalized radiance for wavelength region $\lambda$ and $L_\lambda$ is the measured reflected radiance for wavelength region $\lambda$. Pixels that are in self-shadow have a $\cos(i)$ of less than or equal to 0.0 (i.e., $i \geq 90$ degrees).

Implementation of the Lambertian normalization model is a logical extension of the DEM surface orientation comparison model (Figure 3a). Because the denominator in Equation 11 requires the $\cos(i)$ rather than $i$, the arc cosine function is not used. The grid layer of $\cos(i)$ values is used to normalize each image band on a band-by-band basis (Figure 4b). As in the shaded relief model, the solar elevation and azimuth are scalars.

A commonly used non-Lambertian topographic normalization model was developed by Minnaert (1941). Although the Minnaert-based model was developed for lunar surfaces, it has been applied in numerous remote sensing studies of Earth resources. This model may be expressed in linear form as

$$Ln_\lambda = \frac{L_\lambda * \cos(e)}{\cos^k(i) * \cos^k(e)} \tag{12}$$

where $\cos(e)$ is the exitance angle or slope and $k$ is the Minnaert constant. The Minnaert constant $k$ is often assumed to vary by land-cover class and wavelength (Smith *et al.*, 1980). Under this assumption, the Minnaert constant $k$ for a class is derived from a set of sample pixels of the same class using a linear regression form of Equation 12.

Similar to the implementation of the Lambertian model, the Minnaert-based normalization model requires only a local operation (Figure 4c). This model does require the use of a surface slope layer and a grid of $k$ values by zone.

## Direct Solar Radiation

The goal in modeling solar radiation of surfaces is to estimate either (1) absolute solar flux or (2) relative solar flux. In climatological applications, the goal is often the former where actual solar flux estimates at the surface are desired. The latter goal of relative solar flux is often sufficient for studying solar radiation as a causal factor in biogeographic spatial patterns. There are many solar radiation models that vary depending on the scale of analysis, general climate of the site, and amount of supporting data. For further reading, the articles by Dubayah and Rich (1995) and Duguay (1993) may be consulted. The dominant factor in solar radiation variability on inclined surfaces in these models is the variability in solar flux from the angle of incidence ($i$). A common form of a simple solar radiation model is expressed (after Garnier and Ohmura, 1968) as

$$I_d = I_0 \int_{H_1}^{H_2} p^m \cos(i)\, dH \tag{13}$$

where $I_d$ is the daily total direct radiation in langleys, $I_0$ is the solar constant (e.g., 2.0 ly/min), $H_1$ and $H_2$ are the beginning and ending hours of daylight, $p$ is the mean zenith path transmissivity (e.g., 0.75), and $m$ is the optical air mass: i.e., sec $Z_s = 1/\cos(Z_s)$. This formula is a simple version of the atmospheric processes and would obviously vary with local meteorological conditions such as rainfall, cloudiness, etc. This formula does not consider the *diffuse* or *reflected* components of illumination. The formula above also does not consider the shadows caused by intervening topography. In areas of very rugged terrain, the persistence of shadows becomes increasingly important and the inclusion of this in a viewshed operation is required.

Computation of the incidence angle differs from the shaded relief and topographic normalization models in that the solar angle varies diurnally and seasonally. Implementation requires the accumulation of the incremental solar flux on each surface element throughout the day and throughout the season of interest (e.g., seasonal or annual). Conceptually, we could derive a surface of incremental flux for each unit in time and then aggregate the layers through a local sum. Even small units of time (e.g., 20 minutes) would result in a large number of layers for a year. For example, considering every hour in a day throughout the year would result in 26,280 layers (365*24*3). An alternative is iteratively to create the layer for time$_t$ (current time), add it to a total solar flux layer, and then recreate the layer for the time$_{t+1}$, etc. Formally, there is no "do while" or "for loop" construct in the cartographic modeling language. Pragmatically though, these constructs do exist in macro languages of Arc/Info AML, Arc/Info Grid, ArcView Avenue, or ERDAS EML.

## Spatial Interpolation of Directional Data

The concepts and formulae presented earlier may be extended to spatial interpolation, or even the resampling problem in rectification/registration of regular tesselations (Atkinson, 1985; Jensen, 1996). We briefly present the nature of the spatial interpolation problem with vector data, in general, and an implementation using concepts presented earlier. For simplicity, the interpolation model for directional data presented here is based on the fundamental general inverse distance weighted model for estimating the scalar value $z'$: i.e.,

$$z' = \frac{\sum_i^k \frac{z_i}{d_i^p}}{\sum_i^k \frac{1}{d_i^p}} \tag{14}$$

where $k$ is the number of neighboring observations and $d_i^p$ is the distance to observation, with exponent $p$.

The choice of a spatial interpolation method is influenced by the characteristics of the phenomena to be estimated and the physical laws of such phenomenon to be maintained. For most interpolation problems, the phenomenon is represented by a scalar field and is relatively simple compared to directional data. Two different characteristics may be of interest with directional data: (1) a grid of directions (and possible velocities) that represents the "most likely" direction or movement of the phenomenon for each point, and (2) a grid that depicts the flow of energy or matter at each point based on the physical laws that govern the flow of such. The former characteristic would be useful for interpolation of sensible properties such as surface aspect or wind direction; the latter is closely related to the concept of flux and density. Modeling of flux and density requires temporal observations and treatment of such as a function of time.

Many phenomena that "move" behave in accordance with certain physical laws. It is well-known that matter cannot be created or destroyed (except in nuclear reactions). This axiom gives rise to the equation of continuity also referred to as the conservation of mass. Basically, this equation states that, for an infinitesimal volume, inequalities in the amount of matter (or energy) entering the volume and the amount of matter (or energy) exiting the volume are resolved as changes in the density of the matter (or energy) for the volume. For many applications, the matter is considered incompressible (e.g., water, tropospheric atmosphere, ice) and, thus, invariant in pressure. Thus, if precise maintenance of the conservation of mass is required, then the interpolation algorithm should guarantee this.

The interpolation methods suggested here do not guarantee that mass is conserved. For such moving phenomena and physical laws, three-dimensional data models are required as well as an iterative algorithm for adjusting the estimated grid values to conformity. Preservation of these characteristics is analogous to a spatial interpolation method such as the pycnophylactic interpolation method for conserving mass (Tobler, 1979). However, the methods suggested below may be said to "lean" toward the conservation of mass (particularly if three-dimensional directions are used). In applications that only require approximate surface movement fields, these methods will suffice. For other static directional data, such as the dispersion of phenomena by surface aspect or a combined slope-aspect directional vector, the suggested interpolation methods satisfy statistical assumptions required for weighted means.

By expressing the directional data as unit vectors (e.g., Equation 1 if three-dimensional) in separate grids as before, spatial interpolation may be implemented by performing separate spatial interpolations for the $x$ and $y$ components (and $z$ if three-dimensional). Kemp (1992) also noted the use of vector endpoints for resampling of vector fields. Equal weighting of all neighboring observations results in an interpolated vector equivalent to the vector $\mathbf{T}_{sum}$ in Equation 4. To implement differential weighting of observations as is common, the mean vector $\mathbf{T}_{2d}$ is interpolated by decomposing the problem into

$$\vec{\mathbf{T}}_{2d} = [x_{\text{interpolated}}, y_{\text{interpolated}}] \tag{15}$$

where

$$x_{\text{interpolated}} = \sum_i^k \frac{x}{d_i^p} \bigg/ \sum_i^k \frac{1}{d_i^p}$$

and

$$y_{\text{interpolated}} = \sum_i^k \frac{y}{d_i^p} \bigg/ \sum_i^k \frac{1}{d_i^p}.$$

Once the $x$ and $y$ components for each directional vector are computed, $x_{\text{interpolated}}$ and $y_{\text{interpolated}}$ are derived using the existing interpolation method (e.g., general inverse distance weighting model) or resampling logic.

For example, the resampling of two-dimensional directional data requires the following steps:

(1) Create a grid of $x$ components from the directional value (Equation 1),
(2) Create a grid of $y$ components from the directional value (Equation 1),
(3) Rectify/register the grid of $x$ values in the conventional manner as a scalar, and
(4) Rectify/register the grid of $y$ values in the conventional manner as a scalar; then
(5) Each location in the resulting grids contain the endpoints of the interpolated directional data.

## Discussion

The representation of surface orientation angles in a DEM as a map layer of hemispherically directed vectors puts many surface orientation applications in a broader context (Figure 5). A common foundation for linking these applications mathematically and conceptually through linear algebra and cartographic modeling has been presented. This article has demonstrated that seemingly complex models based on directional concepts can be easily implemented in the existing cartographic modeling language of a modern GIS. Reliance on external "coupled" models is not necessary except for *efficiency* reasons.

As conceptual modeling in a GIS framework continues to evolve, it is imperative that two-and-one-half-dimensional and three-dimensional data models and operators be developed. The representation of two-and-one-half-dimensional surfaces are possible while three-dimensional representations are less well developed. This article has presented concepts and cartographic modeling implementations that are possible through the present evolutionary status for a modern GIS. For efficiency and conceptualization reasons, it might be desirable to organize the surfaces of $x$, $y$, and $z$ components into an "object," as in object-oriented representations. In this manner, references to a "surface orientation object" would refer to the $x$, $y$, and $z$ components of a map layer of unit vectors. Data structures like ERDAS Imagine's multiple layer "images" are an example. As noted earlier, the new vector data object in ESRI's ArcView "3-D Analyst" provides a vector data object, but not for regular tesselations. However, creating a new data type, such as a vector object, only provides an efficient method for encapsulating multiple attributes for a surface. To develop the models discussed in this paper would require the availability of *2½D operators* or *3D operators*, such as vector addition, vector differences, dot and cross products, and higher level concepts like directional statistics.

A comprehensive extension of the cartographic modeling language to three dimensions would require consideration of operators well-beyond the limited scope of surface orientation and sun-surface rays. However, the implementation of "surface orientation objects" (expressed in $x$, $y$, and $z$ components) and associated directional operators with these objects would satisfy the fundamental applications presented here. The following operators (expressed as map algebra statements) would be needed:

- *Grid_Vobject = Vcomponents (grid_DEM)*
- *Grid_Vobject = FocalVmean (window, Grid_Vobject)*
- *Grid_Vobject = ZonalVMean (zone Grid, Grid_Vobject)*
- *Grid = Vslope (Grid_Vobject)*
- *Grid = Vaspect (Grid_Vobject)*
- *Grid = FocalVstd (window, Grid_Vobject)*
- *Grid = ZonalVstd (zone Grid, Grid_Vobject)*
- *Grid = LocalVdiff (Grid_Vobject 1, Grid_Vobject 2)*

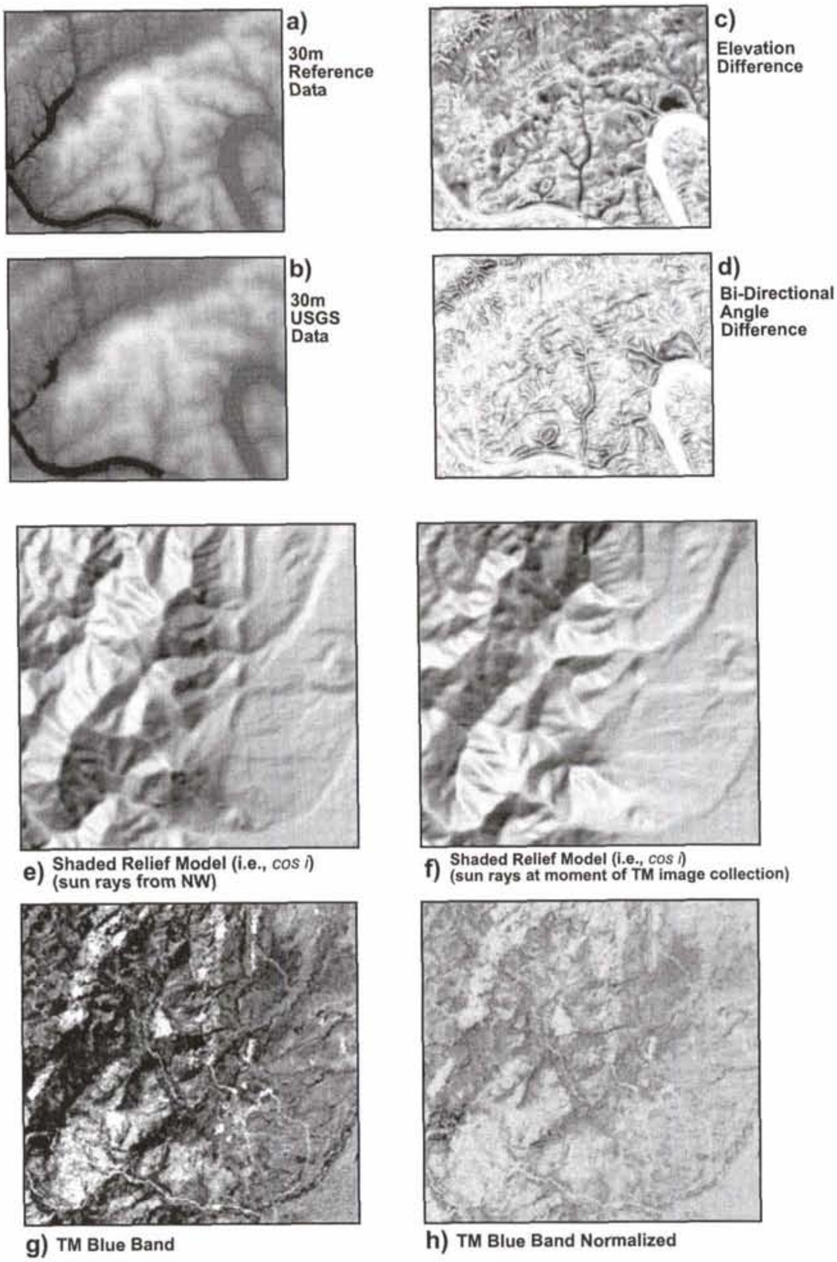


Figure 5. Example applications using the directional operators and models developed. Simple elevation differences between a very high resolution photogrammetrically derived DEM (a) and the USGS 30-m DEM for the same area (b) indicates larger differences in the stream channels and a few other areas (c). The local bi-directional surface angles between the two DEMs (d) highlight the differences in surface orientation adjacent to stream channels. A traditional shaded relief map for an area in Colorado (e) is compared to the surface illumination at the moment of TM image collection (f). The blue band from Landsat TM is shown in (g) and after topographic normalization in (h).

In the above operators, a "grid" is the traditional grid data model of one layer. The *Vcomponents* operator would create the multilayer grid vector object (i.e., *Grid* — *Vobject*) of *x*, *y*, and *z* components from a digital elevation model (i.e., Equation 1). The mean vector ($\mathbf{T}_{sum}$) for a neighborhood or zone could then be derived by *focalVmean* or *zonalVmean* operators, respectively (i.e., Equation 4). A *window* object would describe the size, shape, and specific row-column elements to be used in the focal operation. Slope or aspect for the surface object is derived by the *Vslope* and *Vaspect* operators (i.e., Equation 5), respectively. These two slope and aspect operators differ from the traditional slope/aspect operators in that they derive surface angles from the vector representation rather than the surface elevations in a DEM. The standard deviation in surface orientation ($s_h$) is derived with the *focalVstd* or *zonalVstd* operators. The angle *i* between two vectors in 3D space may be computed using the *localVdiff* operator (i.e., after Equation 3).

There are no formal constructs for "*looping*" to model temporal processes in the cartographic modeling language. Although this prohibits an elegant solution to creating temporal models, looping constructs for modeling temporal processes can be implemented with existing "flow-of-control" constructs available in modern GISs.

No formalized methods exist in GIS languages for modeling flux or density. Preserving these characteristics in modeling applications requires the conservation of mass and energy. Even the methods for spatial interpolation or computation of mean wind direction as presented here (or similar concepts by others) does not insure conservation — these methods only "lean" toward such properties.

Finally, there is also no formalized method for *encapsulation* of modeling code segments into operators (i.e., grey boxes), such as those proposed above. For instance, it would be preferable to build a model for mean surface dispersion based on the available objects and hemispherical operators, and to later use this model by simple reference to a surface dispersion "object" (e.g., *focalVstd* or *zonalVstd*). Existing implementations must rely on separation of embedded models using separate script files (e.g., AML or EML files, or Avenue code) or graphical models.

As the conceptual development of modeling language constructs continues, a standardized modeling language that includes the directional nature of $2^1/_2$D or 3D surface operators will ultimately be accepted by the GIS community. Ideally, modeling language operators for conservation will also be adopted. The conceptual development of surface operators based on cartographic modeling constructs proposed in this article is one approach toward this goal.

## Acknowledgments
The authors would like to express appreciation to Dana Tomlin, David Cairns, Dale Quattrochi, and James Zack for their comments on previous versions of the material in this article. We also recognize the efforts of Dale Quattrochi and Pete Atkinson in this Special Issue of *PE&RS*. The implementation of the constructs in this article as Avenue scripts may be freely obtained on the Internet at *http://www.cla.sc.edu/geog/geogdocs/departdocs/facdocs/hodgson.html*.

## References

Atkinson, P., 1985. Preliminary results of the effect of resampling on Thematic Mapper imagery, *Technical Papers of the ACSM-ASPRS Fall Conference*, pp. 929–936.

Berry, J., 1987. Fundamental operations in computer-assisted map analysis, *International Journal of Geographical Information Systems*, 1:119–136.

Bolstad, P.V., and T. Stowe, 1994. An evaluation of DEM accuracy: elevation, slope, and aspect, *Photogrammetric Engineering & Remote Sensing*, 60(11):1327–1332.

Civco, D.L., 1989. Topographic normalization of landsat thematic mapper digital imagery, *Photogrammetric Engineering & Remote Sensing*, 55(9):1303–1309.

Colby, J.D., 1991. Topographic normalization in rugged terrain, *Photogrammetric Engineering & Remote Sensing*, 57(5):531–537.

Dubayah, R., and P.M. Rich, 1995. Topographic solar radiation models for GIS, *International Journal of Geographical Information Systems*, 9(4):405–419.

Duguay, C.R., 1993. Radiation modeling in mountainous terrain: Review and status, *Mountain Research and Development*, 13:339–357.

Gaile, G.L., and J.E. Burt, 1980. *Directional Statistics*, University of East Anglia, Norwich, 39 p.

Gallant, J.C., and J.P. Wilson, 1996. TAPES-G: A grid based terrain analysis program for the environmental sciences, *Computers and Geosciences*, 22(7):713–722.

Garnier, B.J., and A. Ohmura, 1968. A method of calculating the direct shortwave radiation income of slopes, *Journal of Applied Meteorology*, 7:796–800.

Hanson, B., K. Klink, K. Matsuura, S.M. Robeson, and C.J. Willmott, 1992. Vector correlation: Review, exposition, and geographic application, *Annals of the Association of American Geographers*, 82(1):103–116.

Hodgson, M.E., 1995. What cellsize does the computed slope/aspect angle represent? *Photogrammetric Engineering & Remote Sensing*, 60(5):513–517.

———, 1998. Comparison of bi-directional angles from surface slope/aspect algorithms, *Cartography and Geographic Information Systems*, 25(3):173–187.

Hodgson, M.E., and G. Gaile, 1996. Characteristic mean and dispersion in surface orientations for a zone, *International Journal of Geographical Information Systems*, 10(7):817–830.

Holben, B.N., and C.O. Justice, 1980. The topographic effect on spectral response from nadir-pointing sensors, *Photogrammetric Engineering & Remote Sensing*, 46(9):1191–1200.

Jensen, J.R., 1996. *Introductory Digital Image Processing: A Remote Sensing Perspective, Second Edition*, Prentice-Hall, Inc., Saddle River, New Jersey, 318 p.

Kemp, K., 1992. *Environmental Modeling with GIS: A Strategy for Dealing with Spatial Continuity*, unpublished PhD dissertation, University of California, Santa Barbara.

Klink, K., 1998. Complimentary use of scalar, directional, and vector statistics with an application to surface winds, *The Professional Geographer*, 50(1):3–13.

Mahan, R.P., 1991. *Circular Statistical Methods: Applications in Spatial and Temporal Performance Analysis*, U.S. Army Research Institute for the Behavioral and Social Sciences, Alexandria, Virginia.

Minnaert, M., 1941. The reciprocity principle in lunar photometry, *Astrophysical Journal*, 93:403–410.

Rayleigh, 1880. On the resultant of a large number of vibrations of the same pitch or arbitrary pause, *Philosophical Magazine*, 10: 73–78.

Ritter, P., 1987. A vector-based slope and aspect generation algorithm, *Photogrammetric Engineering & Remote Sensing*, 53: 1109–1111.

Sharpnack, D.A., and G. Akin, 1969. An algorithm for computing slope and aspect from elevations, *Photogrammetric Engineering*, 35:247–248.

Skidmore, A.K., 1989. A comparison of techniques for calculating gradient and aspect from a gridded digital elevation model, *International Journal of Geographical Information Systems*, 3:323–334.

Smith, J., T. Lin, and K. Ranson, 1980. The Lambertian assumption and Landsat data, *Photogrammetric Engineering & Remote Sensing*, 46(9):1183–1189.

Tobler, W.R., 1979. Smooth pycnophylactic interpolation for geographic regions, *Journal of American Statistical Association*, 74(367):519–536.

Tomlin, C.D., 1990. *Geographic Information Systems and Cartographic Modeling*, Prentice-Hall, Englewood Cliffs, New Jersey, 249 p.

Tomlin, C.D., and J.K. Berry, 1979. A mathematical structure for cartographic modeling in environmental analysis, *Proceedings of the Annual Meeting of the American Congress on Surveying and Mapping and the American Society of Photogrammetry*, pp. 269–283.

Wesseling, C.G., D-J. Karssenberg, P.A. Burrough, and W.P.A. Van Deursen, 1996. Integrating dynamic environmental models in GIS: The development of a dynamic modelling language, *Transactions in GIS*, 1(1):40–48.

Yoeli, P.Y., 1986. Shadowed contours with computer and plotter, *The American Cartographer*, 10(2):101–110.

Zhang, Z., and D.A. Griffith, 1997. Developing user-friendly spatial statistical analysis modules for GIS: An example using ArcView, *Computers, Environment, and Urban Systems*, 21(1):5–29.